Thermochimica Acta, 143 (1989) 93–100
Elsevier Science Publishers B.V., Amsterdam – Printed in The Netherlands

KINETIC STUDIES BY DSC ON THE THERMAL DECOMPOSITION OF CALCIUM OXALATE

R. LOZANO *, J. ROMAN and F. DE JESUS

Departamento de Química Inorgánica y Bioinorgánica, Facultad de Farmacia,
Universidad Complutense, 28040 Madrid (Spain)

A. JEREZ, M. GAITAN and E. RAMOS

Departamento de Química Inorgánica, Facultad de C. Químicas, Universidad Complutense,
28040 Madrid (Spain)

(Received 28 June 1988)

ABSTRACT

In the present paper, we have studied the kinetics of the thermal decomposition of calcium oxalate monohydrate, using a new method of kinetic study employing data obtained from differential scanning calorimetry, as previously proposed by us.

Initial products and those obtained following decomposition have been identified by infrared spectroscopy and X-ray powder diffraction.

A comparison between the results obtained in this paper and those reported in the literature has also been made.

INTRODUCTION

The determination of kinetic parameters by non-isothermal methods offers advantages over conventional isothermal studies [1].

However, the methods usually employed for kinetic analyses [2–9] lead to ambiguous results, especially if the reaction studied is diffusion controlled.

In other papers, we have reported on kinetic studies of several molybdenum(IV) and vanadium(IV) complexes using the procedure of Thomas and Clarke [10–12]. However, the results obtained are only over a small portion of the range of the reaction.

Recently, we have reported on a new method of studying the kinetics of non-isothermal decomposition reactions of solids using DSC [13,14].

The object of the present paper is to demonstrate the validity of the proposed method using a well-known highly purified inorganic product,

---

* Author to whom all correspondence should be addressed.

whose kinetic parameters have been previously studied by other workers [3,15].

The thermal decomposition of $CaC_2O_4 \cdot H_2O$ occurs with the loss of H_2O and CO molecules as shown in reactions 1 and 2 respectively

$$CaC_2O_4 \cdot H_2O \rightarrow CaC_2O_4 + H_2O \tag{1}$$

$$CaC_2O_4 \rightarrow CaCO_3 + CO \tag{2}$$

EXPERIMENTAL

Analyses of compounds

The $CaC_2O_4 \cdot H_2O$ is a commercial product of C. Erba, RPE quality, and was used as supplied.

Infrared spectra were determined on a Perkin–Elmer spectrophotometer model 283 using KBr pellets.

The X-ray diffraction was carried out on a Siemens Cristalloflex model D-500 using Cu $K\alpha$ radiation.

Thermogravimetric analysis

Thermogravimetric analysis was performed on a Mettler HE-20 thermobalance. The constants were: heating rate, 5 °C min^{-1}; TG range, 5 mV; chart speed, 20 cm h^{-1}; sample mass, 5 mg; reference, Al_2O_3; and thermocouple, Pt/Pt–Rh 80%.

The analysis was made in a dynamic nitrogen atmosphere between 25 and 600 °C. A platinum pan was used.

Differential scanning calorimetry

Differential scanning calorimetry was performed using a Mettler TA 3000 system with a Mettler DSC-20 differential scanning calorimeter.

The scanning rate used was 5 °C min^{-1} and samples of about 5 mg were used so as to render insignificant the temperature non-uniformity within the sample. An aluminium pan was used under a dynamic nitrogen atmosphere. The instrument calibration was checked periodically with standard samples of indium (99.99% purity). Several runs were made in all cases.

RESULTS AND DISCUSSION

The DSC curve of $CaC_2O_4 \cdot H_2O$ shows an endothermic peak between 126 and 196 °C and an exothermic process between 452 and 500 °C (Fig. 1).

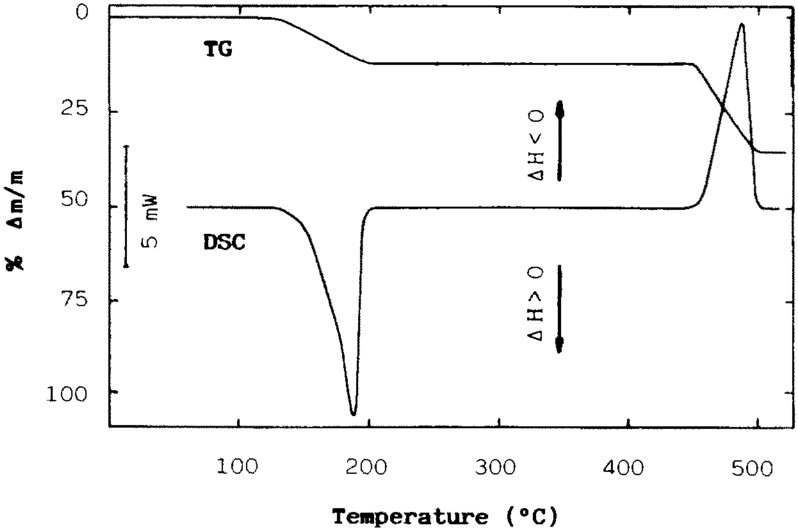

Fig. 1. DSC and TG curves of $CaC_2O_4 \cdot H_2O$.

TABLE 1

ΔH, α, T and α' values obtained from the DSC curve of $CaC_2O_4 \cdot H_2O$

ΔH (mJ)	α (K^{-1})	T (°C)	α' (K^{-1})
79.91	0.0504	152.0	0.0069
99.81	0.0630	154.0	0.0080
123.47	0.0780	156.0	0.0093
150.85	0.0952	158.0	0.0107
182.24	0.1151	160.0	0.0124
217.35	0.1373	162.0	0.0142
256.99	0.1623	164.0	0.0162
302.41	0.1910	166.0	0.0185
353.14	0.2230	168.0	0.0210
410.67	0.2594	170.0	0.0237
474.55	0.2997	172.0	0.0267
547.81	0.3460	174.0	0.0297
626.37	0.3956	176.0	0.0329
715.36	0.4519	178.0	0.0361
811.71	0.5127	180.0	0.0391
918.22	0.5800	182.0	0.0416
1032.10	0.6519	184.0	0.0434
1154.30	0.7292	186.0	0.0439
1285.50	0.8120	188.0	0.0418
1415.20	0.8939	190.0	0.0358
1527.00	0.9646	192.0	0.0236

TABLE 2

Kinetic equations

Mechanism (rate-controlling process)	$f(\alpha)$
D1 (One-dimensional diffusion)	$\frac{1}{2}\alpha$
D2 (Two-dimensional diffusion)	$[-\ln(1-\alpha)]^{-1}$
D3 (Three-dimensional diffusion: Jander equation)	$\frac{3}{2}(1-\alpha)^{2/3}[1-(1-\alpha)^{1/3}]^{-1}$
D4 (Three-dimensional diffusion: Ginstling–Brounshtein equation)	$3/[2(1-\alpha)^{1/3}-1]$
F1 (Random nucleation)	$1-\alpha$
R2 (Phase-boundary reaction: cylindrical symmetry)	$2(1-\alpha)^{1/2}$
R3 (Phase-boundary reaction: spherical symmetry)	$3(1-\alpha)^{2/3}$

The mass loss accompanying the first transition corresponds on the TG curve, to the loss of the H_2O molecule; X-ray powder diffraction identified the product as anhydrous calcium oxalate. The next exothermic process corresponds to the loss of CO, the residue being identified as $CaCO_3$, by infrared spectroscopy and X-ray powder diffraction. Table 1 shows the data for the first transition, obtained from the DSC curve.

Using the mechanisms reported in the literature [1] (see Table 2), we have plotted $(\Delta \ln \alpha' - \Delta \ln f(\alpha))/\Delta \ln(1-\alpha)$ versus $\Delta(1/T)/\Delta \ln(1-\alpha)$, showing the results for r (the correlation coefficient), m (the slope), i (the intercept value) and E_a (the activation energy), obtained for the seven mechanisms (Table 3).

It can be seen that only when the analysis was performed with the R2 mechanism [phase boundary reaction: cylindrical symmetry], was the intercept value close to zero (see Table 3), with an E_a value of 118.00 kJ mol^{-1}.

In order to test the validity of the above conclusions, we have substituted the seven forms of $f(\alpha)$ into the Arrhenius equation in logarithmic form, obtaining eqn. (3)

$$\ln \alpha' = \ln(A/\beta) - E_a/RT + \ln f(\alpha)$$

or

$$\ln \alpha' - \ln f(\alpha) = \ln(A/\beta) - E_a/RT \qquad (3)$$

The plot of $(\ln \alpha' - \ln f(\alpha))$ versus $1/T$ should be a straight line with a slope of $-E_a/R$ and an intercept value of $\ln(A/\beta)$. If the proposed mechanism is correct, the activation energy value should be the same as that obtained previously, as, in fact, is the case. Table 4 shows the values of the activation energy for both analyses, corresponding to the dehydration of $CaC_2O_4 \cdot H_2O$. Only the R2 mechanism shows a very good agreement.

TABLE 3

Results obtained using the seven mechanisms for the plot of $(\Delta \ln \alpha' - \Delta \ln f(\alpha))/\Delta \ln(1-\alpha)$ versus $\Delta(1/T)/\Delta \ln(1-\alpha)$ for $CaC_2O_4 \cdot H_2O$

Mechanism D1
Correlation coefficient, $r = -0.9982$
Slope, $m = -33962.60$
Intercept value, $i = 1.1604$
Activation energy, $E_a = 282.37$ kJ mol^{-1}

Mechanism D2
Correlation coefficient, $r = -0.9984$
Slope, $m = -34120.59$
Intercept value, $i = 0.7510$
Activation energy, $E_a = 283.69$ kJ mol^{-1}

Mechanism D3
Correlation coefficient, $r = -0.9984$
Slope, $m = -34102.03$
Intercept value, $i = 0.2405$
Activation energy, $E_a = 283.53$ kJ mol^{-1}

Mechanism D4
Correlation coefficient, $r = -0.9984$
Slope, $m = -34101.95$
Intercept value, $i = 0.5738$
Activation energy, $E_a = 283.53$ kJ mol^{-1}

Mechanism F1
Correlation coefficient, $r = -1.0000$
Slope, $m = -14193.39$
Intercept value, $i = -0.5000$
Activation energy, $E_a = 118.00$ kJ mol^{-1}

Mechanism R2
Correlation coefficient, $r = -1.0000$
Slope, $m = -14193.39$
Intercept value, $i = -0.0003$
Activation energy, $E_a = 118.00$ kJ mol^{-1}

Mechanism R3
Correlation coefficient, $r = -1.0000$
Slope, $m = -14193.39$
Intercept value, $i = -0.1666$
Activation energy, $E_a = 118.00$ kJ mol^{-1}

Therefore, the process of thermal dehydration of $CaC_2O_4 \cdot H_2O$ follows mechanism R2 (phase boundary reaction: cylindrical symmetry), and the values of the reaction order, the activation energy and the pre-exponential Arrhenius factor are 0.50, 118.00 kJ mol^{-1} and 6.597×10^{11} s^{-1} respectively.

These values, obtained using the proposed method, are in agreement with those previously reported by other workers [3,15].

TABLE 4

Activation energy values obtained by using the seven mechanisms for $CaC_2O_4 \cdot H_2O$

Mechanism	E_a [a] (kJ mol^{-1})	E_a [b] (kJ mol^{-1})	Difference (%)
D1	282.37	192.83	31.71
D2	283.69	230.14	18.87
D3	283.53	276.87	2.34
D4	283.53	246.37	13.10
F1	118.00	163.76	−38.77
R2	118.00	118.02	−0.01
R3	118.00	133.26	−12.93

[a] Calculated from the plot of $[\Delta \ln \alpha' - \Delta \ln f(\alpha)]/\Delta \ln(1-\alpha)$ versus $\Delta(1/T)/\Delta \ln(1-\alpha)$.

[b] Calculated from the plot of $\ln \alpha' - \ln f(\alpha)$ versus $1/T$.

TABLE 5

ΔH, α, T and α' obtained from the DSC curve of CaC_2O_4

ΔH (mJ)	α (K^{-1})	T (°C)	α' (K^{-1})
141.56	0.0828	465.0	0.0155
166.40	0.0974	466.0	0.0168
192.42	0.1126	467.0	0.0181
221.64	0.1297	468.0	0.0194
251.54	0.1472	469.0	0.0209
286.15	0.1675	470.0	0.0224
321.10	0.1880	471.0	0.0240
359.92	0.2107	472.0	0.0256
399.08	0.2336	473.0	0.0274
442.95	0.2593	474.0	0.0291
487.67	0.2855	475.0	0.0309
536.26	0.3140	476.0	0.0327
586.36	0.3433	477.0	0.0346
639.33	0.3743	478.0	0.0364
693.81	0.4062	479.0	0.0382
752.51	0.4406	480.0	0.0399
812.89	0.4759	481.0	0.0415
877.14	0.5136	482.0	0.0429
944.43	0.5530	483.0	0.0440
1016.10	0.5949	484.0	0.0447
1088.30	0.6372	485.0	0.0451
1161.80	0.6802	486.0	0.0450
1236.00	0.7237	487.0	0.0443
1311.00	0.7676	488.0	0.0428
1380.80	0.8085	489.0	0.0408
1446.40	0.8469	490.0	0.0381
1502.60	0.8789	491.0	0.0352
1555.20	0.9106	492.0	0.0313
1597.20	0.9352	493.0	0.0273

TABLE 6

Results obtained using the seven mechanisms for the plot of $(\Delta \ln \alpha' - \Delta \ln f(\alpha))/\Delta \ln(1-\alpha)$ versus $\Delta(1/T)/\Delta \ln - \alpha)$ for CaC_2O_4

Mechanism D1
Correlation coefficient, $r = -0.9936$
Slope, $m = -129688.2$
Intercept value, $i = 1.49303$
Activation energy, $E_a = 1078.28$ kJ mol^{-1}

Mechanism D2
Correlation coefficient, $r = -0.9943$
Slope, $m = -131004.1$
Intercept value, $i = 1.10922$
Activation energy, $E_a = 1089.22$ kJ mol^{-1}

Mechanism D3
Correlation coefficient, $r = -0.9942$
Slope, $m = -130850.5$
Intercept value, $i = 0.5957$
Activation energy, $E_a = 1087.94$ kJ mol^{-1}

Mechanism D4
Correlation coefficient, $r = -0.9942$
Slope, $m = -130850.3$
Intercept value, $i = 0.9291$
Activation energy, $E_a = 1087.94$ kJ mol^{-1}

Mechanism F1
Correlation coefficient, $r = -1.0000$
Slope, $m = -47073.64$
Intercept value, $i = -0.3333$
Activation energy, $E_a = 391.38$ kJ mol^{-1}

Mechanism R2
Correlation coefficient, $r = -1.0000$
Slope, $m = -47073.66$
Intercept value, $i = 0.1666$
Activation energy, $E_a = 391.38$ kJ mol^{-1}

Mechanism R3
Correlation coefficient, $r = -1.0000$
Slope, $m = -47073.62$
Intercept value, $i = -0.0002$
Activation energy, $E_a = 391.38$ kJ mol^{-1}

In Table 5, we list the data for the process of decarbonylation of CaC_2O_4. Table 6 shows r, m, i and E_a values for the seven mechanisms tested.

It can be seen that only the R3 mechanism (phase boundary reaction: spherical symmetry) has an intercept value close to zero, with an E_a value of 391.38 kJ mol^{-1}.

TABLE 7

Activation energy values obtained using the seven mechanisms for CaC_2O_4

Mechanism	E_a [a] (kJ mol^{-1})	E_a [b] (kJ mol^{-1})	Difference (%)
D1	1078.28	542.86	49.65
D2	1089.22	697.87	35.92
D3	1087.94	889.17	18.27
D4	1087.94	764.13	29.76
F1	391.38	516.42	−31.94
R2	391.38	328.88	15.96
R3	391.38	391.39	0.00

[a] Calculated from the plot of $[\Delta \ln \alpha' - \Delta \ln f(\alpha)]/\Delta \ln(1-\alpha)$ versus $\Delta(1/T)/\Delta \ln(1-\alpha)$.
[b] Calculated from the plot of $\ln \alpha' - \ln f(\alpha)$ versus $1/T$.

When we test our method by plotting $\ln \alpha' - \ln f(\alpha)$ versus $1/T$, we obtain new values for the activation energy, as shown in Table 7, compared with the E_a values previously calculated. The R3 mechanism shows only a slight percentage difference in E_a value.

Therefore, the process of thermal decarbonylation of calcium oxalate is controlled by mechanism R3 (phase boundary reaction: spherical symmetry); the reaction order, consequently, is 0.66, the activation energy is 391.38 kJ mol^{-1} and the pre-exponential Arrhenius factor has a value of 8.611×10^{24} s^{-1}.

REFERENCES

1 W.W. Wendlandt, Thermal Methods of Analysis, Wiley, New York, 1974.
2 A.E. Nerwkirk, Anal. Chem., 32 (1960) 1558.
3 E.S. Freeman and B. Carroll, J. Phys. Chem., 62 (1958) 394.
4 A. Jerez, J. Therm. Anal., 26 (1983) 315.
5 H.H. Horowitz and G. Metzger, Anal. Chem., 35 (1963) 1464.
6 A.W. Coats and J.P. Redfern, Nature, 201 (1964) 68.
7 C.D. Doyle, J. Appl. Polymer. Sci., 5 (1961) 285.
8 T.R. Ingraham and P. Marrier, Can. J. Chem. Eng., (1964) 161.
9 B.N.N. Achar, G.W. Brindley and J.H. Sharp, Proc. Int. Clay Conf., Jerusalem, 1, (1966) 67.
10 J.M. Thomas and T.A. Clarke, J. Chem. Soc. A, (1968) 457.
11 R. Lozano, J. Martínez, A. Martínez and A. Doadrio, Polyhedron, 2 (1983) 99; 108 (1986) 1.
12 R. Lozano, J. Roman and A. Moragues, Thermochim. Acta, 108 (1986) 1.
13 R. Lozano, J. Román, A. Moragues, A. Jerez and E. Ramos, Transition Met. Chem., 12 (1987) 289.
14 R. Lozano, J. Román, F. de Jesús, A. Jerez, M. Gaitán and E. Ramos, Thermochim. Acta, 141 (1989) 261.
15 E. Segal and C. Popescu, Thermochim. Acta, 48 (1981) 383.